J Solid State Electrochem (2009) 13:1171–1179
DOI 10.1007/s10008-008-0632-1

ORIGINAL PAPER

Electrocatalytic oxidation of glucose on Ni and NiCu alloy modified glassy carbon electrode

M. Jafarian · F. Forouzandeh · I. Danaee · F. Gobal · M. G. Mahjani

Received: 5 May 2008 / Revised: 1 July 2008 / Accepted: 17 July 2008 / Published online: 16 August 2008

Abstract Nickel and nickel–copper alloy modified glassy carbon electrodes (GC/Ni and GC/NiCu) prepared by galvanostatic deposition were examined for their redox processes and electro-catalytic activities towards the oxidation of glucose in alkaline solutions. The methods of cyclic voltammetry (CV) and chronoamperometry (CA) were employed. The cyclic voltammogram of NiCu alloy demonstrates the formation of β/β crystallographic forms of the nickel oxyhydroxide under prolonged repetitive potential cycling in alkaline solution. It is also observed that the overpotential for O_2 evolution increases for NiCu alloy modified electrode. In CV studies, NiCu alloy modified electrode yields significantly higher activity for glucose oxidation compared to Ni. The oxidation of glucose was concluded to be catalyzed through mediated electron transfer across the nickel hydroxide layer comprising of nickel ions of various valence states. The anodic peak currents show linear dependency with the square root of scan rate. This behavior is the characteristic of a diffusion-controlled process. Under the CA regime, the reaction followed a Cottrellian behavior, and the diffusion coefficient of glucose was found to be 1×10^{-5} cm^2 s^{-1}, in agreement with diffusion coefficient obtained in CV studies.

Keywords Glucose · Electrocatalysis · Nickel · Modified electrode · Copper

M. Jafarian (✉) · F. Forouzandeh · I. Danaee · M. G. Mahjani
Departement of Chemistry, K. N. Toosi University of Technology,
P. O. Box 15875-4416, Tehran, Iran
e-mail: mjafarian@kntu.ac.ir

F. Gobal
Departement of Chemistry, Sharif University of Technology,
P. O. Box 11365-9516, Tehran, Iran

Introduction

Electrocatalytic processes involving the oxidation of sugars are of great interest in many areas, ranging from medical applications to wastewater treatment and from the construction of biological fuel cells to analytical applications in the food industry [1–4].

The investigation of glucose electrochemical oxidation began in 1960s and has remained a very active research area [5]. Bagotzky and Vassilyev [6] first reported the electro-oxidation of glucose in an acidic medium. At about the same time, Bockris et al. [7] studied this reaction at high temperature in alkaline solutions. In recent years, infrared (IR) spectrometry has been used to examine the adsorption and oxidation of glucose on Pt electrodes. Bae and coworkers [8, 9] used Fourier transform IR spectroscopy to demonstrate for the first time that the main absorbed intermediate in glucose oxidation in both acidic and alkaline solutions is CO, similar to the oxidation of small organic molecules such as CH_3OH, HCOOH, and HCHO. Studies of Pt single-crystal electrodes have shown that this reaction strongly depends on the crystallographic orientation of the electrode surface [10].

Oxidizable metal electrodes, Ni [11–13], Au [14], Pt [15], and Cu [16] provide simple routes for the catalytic oxidation of carbohydrates at constant applied potentials. Fleischmann et al. [17] studied Ni electrodes and explained the oxidation of alcohols and amines on the basis of a mechanism involving electron-transfer mediation by a $Ni(OH)_2$/NiOOH redox couple in the oxide film at the anodized electrode surface. A similar mechanism has been suggested by Luo et al. [18] to explain the anodic oxidation of glucose at Ni electrodes in alkaline media. Pure Cu electrodes have demonstrated activity for the anodic oxidation of carbohydrates in alkaline media. However, the corresponding response mech-

anism remains somewhat controversial. Nevertheless, following the evidence for Ni electrodes, it has been suggested that a Cu(II)/Cu(III) redox couple at the surface of the anodized Cu electrodes can function within an electron-transfer-mediated mechanism for carbohydrate oxidation [19–20].

Motivation for the study of alloy electrodes is derived primarily from the anticipation of a synergistic electrocatalytic benefit from the combined properties of the components of alloys. Furthermore, the use of pre-anodized alloy electrodes is expected to offer the advantage of ease of preparation and long-term stability in comparison with thermally prepared and electrolytically deposited mixed-oxide film electrodes. Kuwana and co-workers investigate the alloy electrodes in carbohydrate oxidation on Ni-based alloys containing high percentages of Cu and Cr [21, 22]. These researchers reported that Ni-containing alloys exhibited promising stabilities for the glucose oxidation.

The fact that the pure Ni and Cu metals have the same face-centered cubic structure with similar lattice parameters (a= 3.523 for Ni and 3.616 for Cu) makes it possible to have a wide range of compositions for NiCu alloys. Numerous papers have described chemical and physical properties of NiCu alloys. An excellent review was presented by Khulbe et al. [23] on the behavior of NiCu alloys in a variety of catalytic reactions including hydrogenation reactions, *ortho-para* hydrogen conversion, and H_2/D_2 exchange reaction.

The purpose of the present work was to study the electrochemical oxidation of glucose on a nickel and nickel–copper alloy modified glassy carbon electrode in a solution of 1 M NaOH.

Materials and methods

Sodium hydroxide, nickel sulfate, copper sulfate, sodium citrate, and glucose used in this work were Merck (Darmstadt, Germany) products of analytical grade and were used without further purifications. Doubly distilled water was used throughout.

Electrochemical studies were carried out in a conventional three-electrode cell powered by an electrochemical system comprising EG&G model 273 potentiostat/galvanostat and Solartron model 1255 frequency response analyzer. The system is run by a PC through M270 and M389 commercial software's via a GPIB interface. A dual Ag/AgCl-Sat'd KCl, a Pt wire and a glassy carbon (GC) disk electrode were used as the reference, counter and working electrodes, respectively. All studies were carried out at 298±2 K.

The GC disk electrode supplied by EG&G was further polished with 0.05-mm alumina powder on a polishing microcloth and rinsed thoroughly with doubly distilled water prior to modification. Films of nickel were formed on the GC surface by galvanostatic deposition from a solution composed of 0.7 M $NiSO_4$ + 0.26 M $C_6H_5Na_3O_7{\cdot}2H_2O$ for Ni deposition at the current density of 10 mA cm^{-2} and for 300 s and addition of 0.05 M $CuSO_4{\cdot}5H_2O$ for NiCu alloy deposition. Working electrode was placed in the middle of the electrolyte, and electrolyte was stirred with magnetic stirrer during electrodeposition. The surface morphology of the deposit was evaluated by metallographic microscope Neophot 32. The chemical composition of the deposit was evaluated by scanning electron microscopy (Philips XL30) equipped with the energy dispersive X-ray (EDX).

Results and discussion

The surface morphology of the electrodeposited Ni and NiCu alloy was investigated by metallographic microscope as displayed in Figs. 1a,b. As can be seen, smooth surfaces are observed for electrodeposited Ni and NiCu alloy. The result of chemical composition analysis obtained by EDX method revealed that the composite contains 79% Ni and 21% Cu. The composition is given in weight percents (Fig. 1c).

Figure 2 presents consecutive cyclic voltammograms (CV) of a nickel electrode in 1 M NaOH solution recorded at a potential sweep rate of 100 mV s^{-1}. In the first sweep, a pair of redox peaks appear at 500 and 405 mV/Ag, AgCl that are assigned to the Ni(II)/Ni(III) redox couple according to:

$$Ni(OH)_2 + OH^- \Leftrightarrow NiOOH + H_2O + e^-$$

In the subsequent cycles, both the anodic and cathodic peaks shift negatively and stabilize, pointing to higher energies (potential) required for nucleation of NiOOH in the first cycle. The enhanced baseline current of the first cycle is associated with the oxidation of Ni to Ni(II) followed by the continued formation of α-$Ni(OH)_2$ film which slowly converts to β-$Ni(OH)_2$. The growth of current with the number of potential scans indicate the progressive enrichment of the accessible electroactive species, Ni(II) and Ni(III), on or near the surface. The current increase following the anodic wave is the result of the oxygen evolution reaction. The intensity of this reaction also slowly grows with advancing polarization, suggesting a correlation between the oxygen evolution and the concentration of Ni(III) sites. After prolonged cycling, the redox peak potential are stabilized at 471 and 388 mV/Ag, AgCl. The changes of the peaks position are likely due to the changes [24–26] in the crystal structures of the nickel hydroxide and the nickel oxyhydroxide constituents of the electrochemically formed surface film. It has been reported [25, 26] that at the initial stages of electro-oxidation, α-$Ni(OH)_2$ forms and is further slowly converted to the β-$Ni(OH)_2$ form. Both the electrodeposited nickel hydroxide and nickel oxyhydroxide phases are believed to be non-stoichiometric [27, 28].

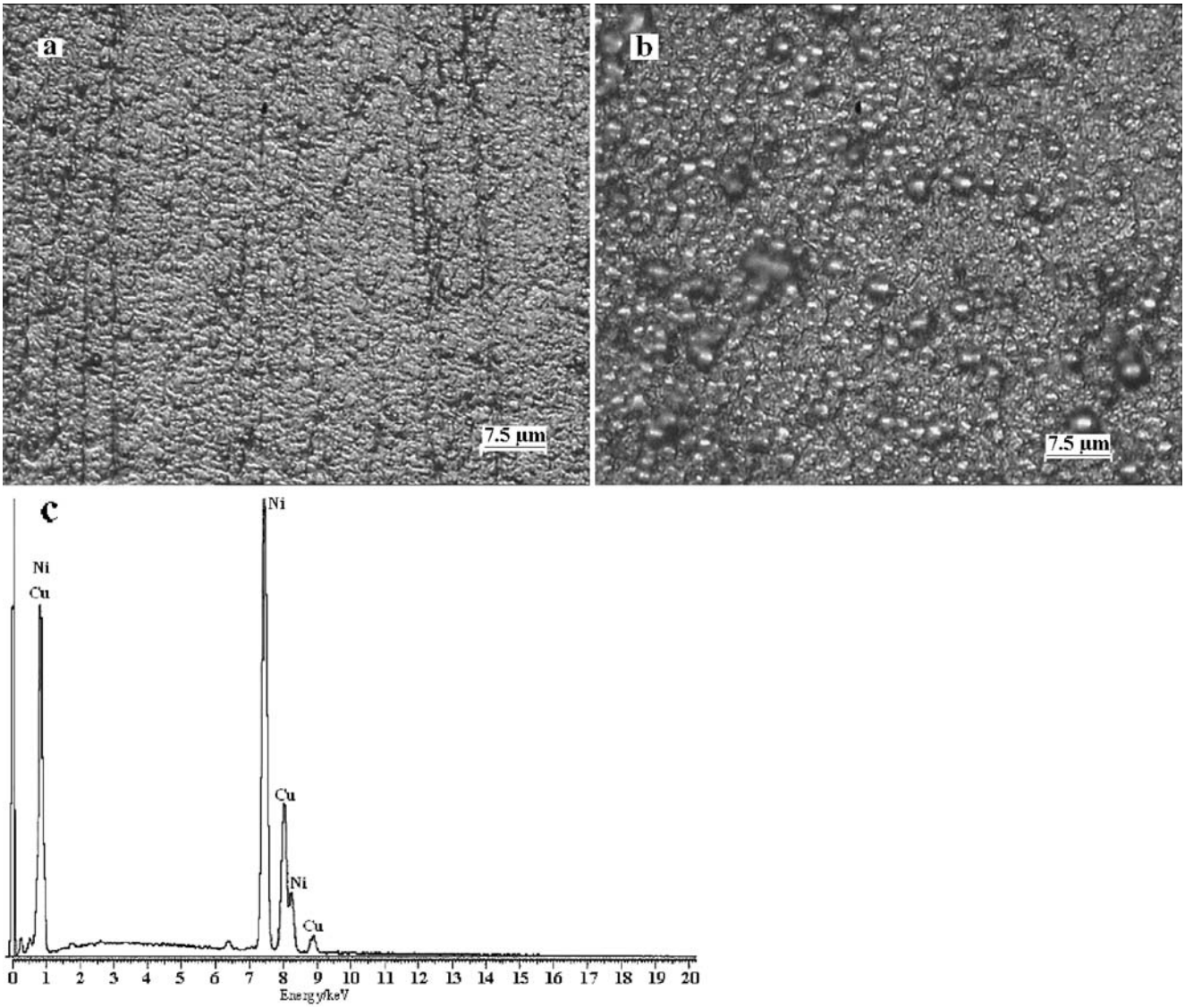

Fig. 1 Metallograph of electrode surface after electrodeposition of Ni (**a**) and NiCu (**b**) alloy from a solution composed of 0.7 M $NiSO_4$ + 0.26 M $C_6H_5Na_3O_7{\cdot}2H_2O$ for Ni deposition at the current density of 10 mA cm^{-2} and for 300 s and addition of 0.05 M $CuSO_4$ for NiCu alloy deposition. (**c**) EDX results of the chemical composition of NiCu alloy at the surface

Figure 3 shows the consecutive CV of a nickel–copper alloy electrode in 1 M NaOH solution recorded at a potential sweep rate of 100 mV s^{-1}. The oxygen evolution reaction is markedly diminished, and its intensity remain unchanged with continued polarization. Ni sites are considered to be responsible for the oxygen evolution reaction [29]. The first positive potential scan reveals a characteristic similar to that of pure Ni, a monotonic current increase in a wide range of potential and a peak shift to a more positive potential. Initially, a $Ni(OH)_2$ layer is formed on the surface of NiCu alloy during the positive potential scan [30]. The rapid formation of $Ni(OH)_2$ at low potential leads to a Cu-rich metal surface which is oxidized to Cu_2O and further to Cu–Cu $(OH)_2$ later [30]. Therefore, the surface layer is subsequently transformed to a mixture of NiOOH and $Cu(OH)_2$ [30]. In addition, some $Cu(OH)_2$ and CuO can be oxidized further to the Cu(III) oxide prior to the evolution of oxygen [31]. The change observed in the current of oxygen evolution may refer in part to the overpotential for the oxygen evolution reaction on copper oxides.

In consecutive cyclic voltammograms of nickel–copper alloy, the peak potentials, except for the first cycle, are invariable, which suggests that the phase transformation of Ni oxyhydroxide from β to γ is inhibited. It is reported that there are four phases produced over the cyclic voltammogram of a nickel hydroxide electrode substrate, namely, β-$Ni(OH)_2$, α-$Ni(OH)_2$, β-NiOOH, and γ-NiOOH [32, 33]. The well-known Bode diagram can be used to identify the phase transfor-

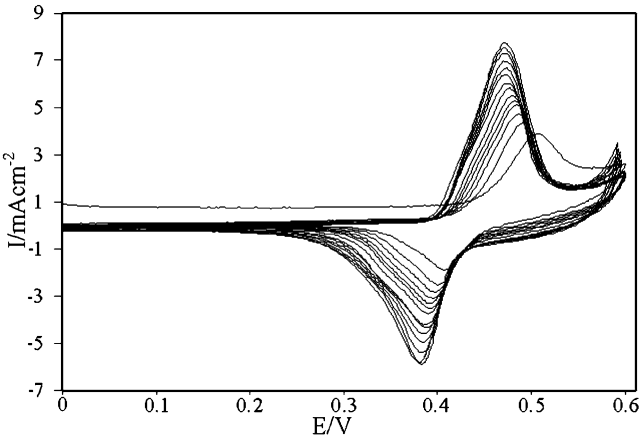

Fig. 2 Consecutive cyclic voltammograms of GC/Ni oxidation in 1 M NaOH at the scan rate of 100 mV s^{-1}. Potential sweep numbers 1 to 50

mations that are likely to occur during a normal potential cycle. β-$Ni(OH)_2$ is first oxidized into β-NiOOH, and the subsequent reduction during the cell discharge can be considered as the intercalation into the β phase of one proton and one electron per Ni atom. Alternatively, γ-NiOOH is reduced into the hydrated α-$Ni(OH)_2$ phase, which is unstable in strong alkali and ages to the β-form. In addition, β-NiOOH is partially converted to γ-NiOOH under experimental conditions of overcharge, high charge/discharge rates, and high alkali concentrations [34, 35]. However, these physical transformations occur slowly and are generally incomplete, so that α/γ and β/β systems coexist under steady-state conditions [35]. It is well known that the formation of γ-NiOOH phase is associated with swelling or volume expansion of nickel film electrodes with subsequent microcracks and disintegrates. Lower interelectrode spacing results in lower internal resistance and therefore better efficiency of the electrode [34, 35]. Therefore, β-NiOOH phase is expected to be a better electroactive material for high electrochemical performance in alkaline solution. The comparison of the electrochemical behavior of the pure electrodeposited nickel and NiCu electrodeposited alloy (see Figs. 2 and 3, respectively) reveals lower α/γ redox contribution with good stabilization of β/β nickel oxyhydroxide on the NiCu electrode. This is due to inhibition of variation of peak potentials after prolonged electrochemical treatment in alkaline solution. Thus, the addition of copper hydroxide to the nickel oxyhydroxide species represents a very efficient strategy of suppressing the formation of γ-NiOOH phase. Similar electrochemical behavior has been observed for Ni-based alloys having several percents of Cd, Zn, Co, Ca, Ti, etc. [34, 36, 37].

Figure 4a presents typical CVs of a GC/NiCu electrode in 1 M NaOH solution at various potential sweep rates of 2 to 2,000 mV s^{-1}. The peak's currents are proportional to sweep rates in the range of 2–40 mV s^{-1} (Fig. 4b, c), pointing to the electrochemical activity of the surface redox couple [38]. From the slope of these lines and using [38]:

$$I_p = \left(\frac{n^2F^2}{4RT}\right)\nu A\Gamma^* \tag{1}$$

where Γ* is the surface coverage of the redox species and ν being the potential sweep rate, and taking average of both cathodic and anodic results, Γ* values of around 5.6×10^{-8} and 7.1×10^{-8} mol cm^{-2} have been derived that correspond to the presence of around 60 and 75 monolayers of surface species for Ni and NiCu electrodes, respectively. In the higher potential sweep rates, this dependency is of square root form (Fig. 4d,e), signifying the dominance of the diffusion-controlled processes.

Laviron [39] derived general expressions for the cyclic voltammetric response for the case of surface-confined electro-reactive species at small concentrations. For $\Delta E_p < 200/n$ mV, where n is the number of exchanged electrons, commonly observed at low scan rates, Laviron [39] provided some working curves allowing determination of α, transfer coefficient, and k_s, charge transfer rate constant. For $\Delta E_p > 200/n$ mV obtained at very high scan rates, the following simplified relations were proposed:

$$E_{pa} = E^o + A\ln\left[\frac{1-\alpha}{m}\right] \tag{2}$$

$$E_{pc} = E^o + B\ln\left[\frac{\alpha}{m}\right] \tag{3}$$

$$\ln k_s = \alpha\ln(1-\alpha) + (1-\alpha)\ln\alpha - \ln\left(\frac{RT}{nFv}\right) - \frac{\alpha(1-\alpha)nF\Delta E_p}{RT} \tag{4}$$

where $A = RT/(1-\alpha)nF$, $B = RT/\alpha nF$, $m = (RT/F)(k_s/n\nu)$, E_{pa} and E_{pc} are anodic and cathodic peak potential, respectively,

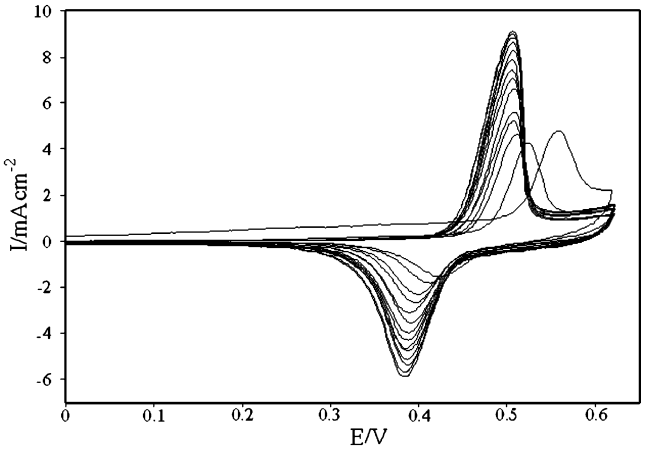

Fig. 3 Consecutive cyclic voltammograms (sweep numbers 1 to 50) of GC/NiCu oxidation in 1 M NaOH at the scan rate of 100 mV s^{-1}

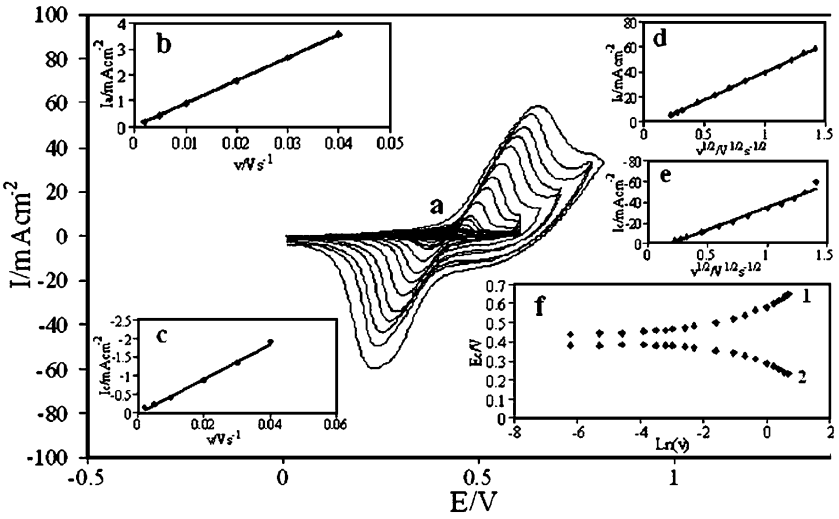

Fig. 4 **a** Typical cyclic voltammograms of a GC/NiCu electrode in 1 M NaOH in the potential sweep rates of 2, 5, 10, 20, 50, 100, 200, 350, 500, 700, 1,000, 1,250, 1,500, 1,750, 2,000 mV s^{-1}. The dependency of anodic (**b**) and cathodic (**c**) peak currents to the sweep rate at lower values (2–40 mV s^{-1}). The proportionality of anodic (**d**) and cathodic (**e**) peak currents to the square roots of sweep rate at higher values (50–2,000 mVs^{-1}). **f** Plot of E_p vs. lnν for cyclic voltammograms depicted in **a** for anodic peaks (*1*) and cathodic peaks (*2*)

and ν the potential sweep rate, respectively. From these expressions, α can be determined by measuring the variation of the peak potential with respect to the potential sweep rate, and k_s can be determined for electron transfer between the electrode and surface modified layer by measuring the E_p values. Figure 4f shows the plot of E_p with respect to the lnν from cyclic voltammograms recorded for GC/NiCu electrode in 1 M NaOH solution at potential sweep rates of 2–2,000 mV s^{-1} for anodic (1) and cathodic (2) peaks. For the potential sweep rates of 200–2,000 mVs^{-1}, the values of E_p are indeed proportional to the logarithm of the potential sweep rate indicated by Laviron. Using the plot and Eq. 4, the values of α were determined as 0.57 and 0.59, and the values of k_s were determined as 0.35 and 0.45 s^{-1} for Ni and NiCu alloy electrodes, respectively. The data reveal a higher electron-transfer rate in the redox process of nickel species present in the modifier film prepared via oxidation of nickel–copper alloy in alkaline solution rather than electrodeposited Ni.

Figure 5 shows cyclic voltammograms of GC/Ni and GC/NiCu electrode in 1 M NaOH solution in the presence of 5 mM glucose at a potential sweep rate of 10 mV s^{-1}. As can be seen in 5 mM glucose, GC/NiCu electrode generates higher current density for the electro-oxidation in NaOH solution due to higher surface concentration of β-NiOOH form.

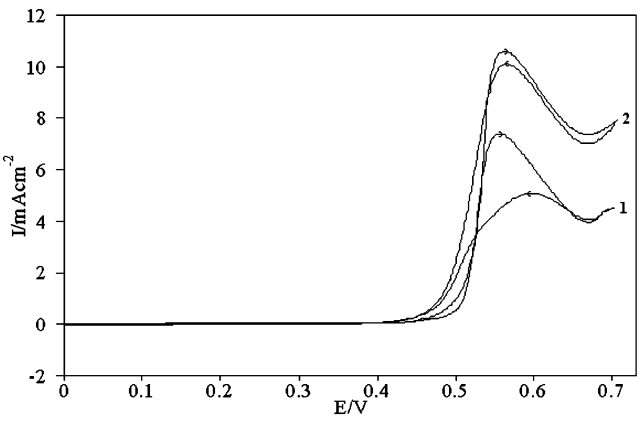

Fig. 5 Cyclic voltammograms of the GC/Ni (*1*) and GC/NiCu (*2*) electrode in 1 M NaOH solution in the presence of 5 mM of glucose in the solution. Potential sweep rate was 10 mV s^{-1}

Figure 6 shows cyclic voltammograms of GC/NiCu electrode in the absence (1) and presence (2) of various concentrations of glucose at a potential sweep rate of 10 mV s^{-1}. At GC/NiCu electrode, oxidation of glucose appeared as a typical electrocatalytic response. The anodic charge increased with respect to that observed for the modified surface in the absence of glucose, and it was followed by decreasing the cathodic charge upon increasing the concentration of glucose in solution. In the presence of 7 mM glucose with the potential sweep rate of 10 mV s^{-1}, the charge associated with the anodic peak was 99% of that of the corresponding cathodic peak, while in the absence of glucose, this ratio was 58%.

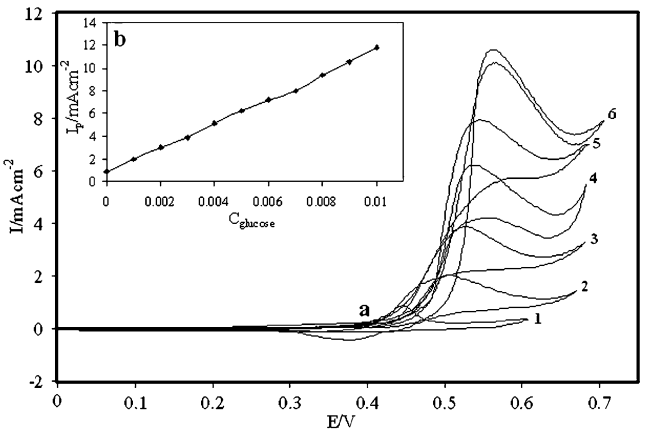

Fig. 6 Cyclic voltammograms of the GC/NiCu electrode in 1 M NaOH solution in the presence of 0 mM (*1*); 1 mM (*2*); 3 mM (*3*); 5 mM (*4*); 7 mM (*5*); 9 mM (*6*) of glucose. Potential sweep rate was 10 mV s^{-1}. *Inset*: Dependency of the anodic peak current on the concentration of glucose in solution

Charge is obtained by integrating the anodic and cathodic peaks under the background correction.

The anodic current in the positive sweep was proportional to the bulk concentration of glucose, and any increase in the concentration of glucose caused an almost proportional linear enhancement of the anodic current (inset Fig. 6). Moreover, in the presence of glucose, the onset potential of the Ni(II) moiety oxidation shifted to positive value and enhanced upon increasing the concentration of glucose. In fact, this indicated a strong interaction of glucose with the surface already covered by low valance nickel species. Therefore, catalytic electro-oxidation of glucose on GC/NiCu seems to be certain.

The decreased cathodic current in the reverse cycle indicated that the rate-determining step certainly involves glucose and that it was incapable of reducing the entire high valent nickel species formed in the oxidation cycle.

The electrocatalytic oxidation of glucose occurs not only in the anodic but also continues in the initial stage of the cathodic half cycle [40]. Glucose molecules adsorbed on the surface are oxidized at higher potentials parallel to the oxidation of Ni(II) to Ni(III) species. The later process has the consequence of decreasing the number of sites for glucose adsorption that, along with the poisoning effect of the products or intermediates of the reaction, tends to decrease the overall rate of glucose oxidation. Thus, the anodic current passes through a maximum as the potential is anodically swept. In the reverse half cycle, the oxidation continues, and its corresponding current goes through a maximum due to the regeneration of active sites for the adsorption of glucose as a result of removal of adsorbed intermediates and products. Due to lower vacant d-orbital of NiCu alloy, desorption of products are easier. Surely, the rate of glucose oxidation as signified by the anodic current in the cathodic half cycle drops as the unfavorable cathodic potentials are approached. In addition, continuous cycling of GC/NiCu in the presence of glucose showed that glucose reacted with the surface, and no poisoning effect on the surface was observed.

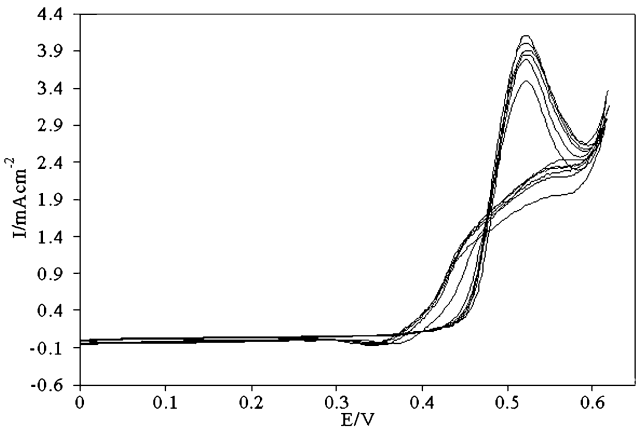

Fig. 7 Repeated cyclic voltammograms of 3 mM glucose oxidation on GC/NiCu electrode at 10 mV s^{-1}, cycle number 1, 10, 20, 50, 100, 150

The redox transition of nickel species present in the film is:

$$\mathrm{Ni(II)} \xleftrightarrow{k_1,k_{-1}} \mathrm{Ni(III)} + e^- \tag{5}$$

and glucose is oxidized on the modified surface via the following reaction:

$$\mathrm{Ni(III)} + \mathrm{glucose} \xrightarrow{k_2} \mathrm{intermediate} + \mathrm{Ni(II)} \tag{6}$$

$$\mathrm{Ni(III)} + \mathrm{intermediate} \xrightarrow{k_3} \mathrm{products} + \mathrm{Ni(II)}. \tag{7}$$

Gluconolactone [11] as well as formats and oxalates [41] have been reported as the oxidation products.

Figure 7 shows the cyclic voltammograms of GC/NiCu electrode in 1 M NaOH in the presence of 3 mM glucose at a scan rate of 10 mV s^{-1} for 150 cycles. It is observed that the current density of the electro-oxidation of glucose is almost constant in 150 cycles, signifying the stability of electrocatalyst.

Cyclic voltammograms of GC/NiCu in the presence of 5 mM glucose at various potential sweep rates and the proportionality of anodic peak currents to the square root of sweep rates in a range of 2 to 2,000 mV s^{-1} are illustrated in Fig. 8a,b, respectively. The cathodic peak was not observed in low scan rates, but appeared upon increasing the sweep rate. The phenomenon indicates that the electro-oxidation of nickel species to higher valence state is much faster than the catalytic oxidation of glucose. This reveals that the oxidation of glucose on Ni may belong to a slow process. In higher scan rates, a new oxidation peak was observed for glucose oxidation at a potential much more positive than that of the oxidation of $Ni(OH)_2$ potential. Meanwhile, the anodic peak currents that are linearly proportional to the square root of scan rate (Fig. 8b) suggests that the overall oxidation of glucose at this electrode is controlled by the diffusion of glucose to the surface redox sites. Moreover, a plot of the so-called current function, $I/v^{1/2}$, with respect to the scan rate (Fig. 8c), exhibited a typical shape of an electrochemical–chemical (EC′) catalytic process [42]. The value of electron transfer coefficient for the reaction which is totally irreversible-diffusion-controlled can be obtained through the following equation [43]:

$$E_P = \left(\frac{RT}{n\alpha F}\right) \ln v + \text{constant}. \tag{8}$$

Using the dependency of anodic peak potential on the natural logarithm of the potential sweep rate (Fig. 8d), the value of electron transfer coefficient was obtained as 0.8.

Setting the working electrode potentials to some selected values, the measurement of the catalytic rate constant as well as the diffusion coefficient of glucose was performed under chronoamperometric regime. Figure 9a shows double step

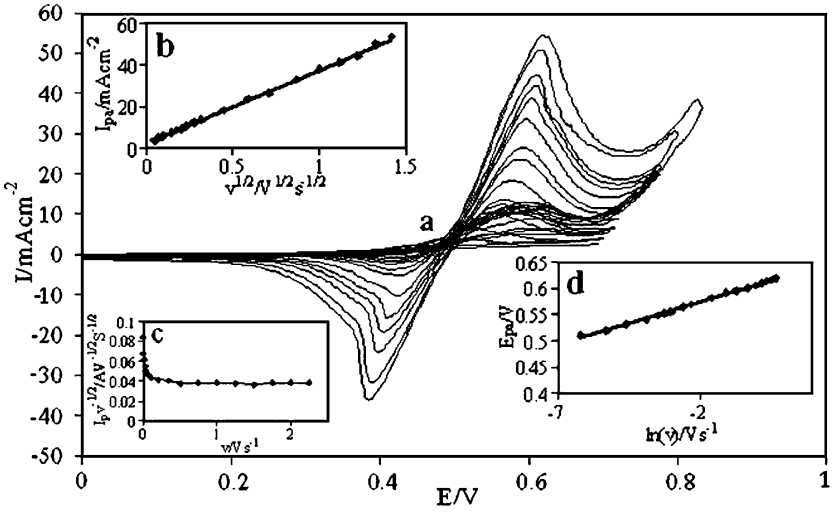

Fig. 8 **a** Typical cyclic voltammograms of the GC/NiCu in1 M NaOH in the presence of 5 mM glucose at various potential sweep rates of 2, 10, 50, 75, 100, 200, 350, 500, 750, 1,000, 1,250, and 1,500 mV s^{-1}. **b** Dependence of anodic peak current during the forward sweep on the square roots of sweep rate. **c** The anodic current function ($I/\nu^{1/2}$) vs. potential sweep rate ν. **d** Dependence of the peak potential on lnν for the oxidation of glucose at GC/NiCu electrode

choronoamperograms for the GC/NiCu in the absence (1) and presence (2–6) of glucose over a concentration range of 1 to 9 mM with applied potential steps of 560 and 320 mV, respectively. Plotting of net current with respect to the inverse of the square roots of time, after removing the background current, presents a linear dependency (Fig. 9b). The dominance of a diffusion-controlled process is evident. Using the slope of this line in Cottrell equation [44]:

$$I = nFAD^{1/2}C^{*}\pi^{-1/2}t^{-1/2} \tag{9}$$

the diffusion coefficient of glucose has been obtained to be 1×10^{-5} cm^2 s^{-1}, which is in good agreement with value reported in the literature [45]. The current is also negligible when potential is stepped down to 320 mV, indicating the irreversibility of glucose oxidation process.

Choronoamperometry can also be used for the evaluation of the catalytic rate constant according to Pariente et al. [46]

$$\frac{I_{\mathrm{cat}}}{I_{\mathrm{L}}} = \gamma^{1/2}\left[\pi^{1/2}\mathrm{erf}\left(\gamma^{1/2}\right) + \frac{\exp(-\gamma)}{\gamma^{1/2}}\right] \tag{10}$$

where I_{cat} and I_{L} are the currents of the GC/NiCu in the presence and absence of glucose and $\gamma = kC^{*}t$ is the argument of the error function. k is the catalytic rate constant, C^{*} is bulk concentration of glucose, and t is elapsed time (s). In the cases where $\gamma > 1.5$, erf($\gamma^{1/2}$) is almost equal to unity, and the above equation simplifies to:

$$\frac{I_{cat}}{I_{L}} = \gamma^{1/2}\pi^{1/2} = \pi^{1/2}(kC^{*}t)^{1/2} \tag{11}$$

From the slope of the $I_{\mathrm{cat}}/I_{\mathrm{L}}$ vs. $t^{1/2}$ plot, presented in Fig. 9c, the mean value of k for the concentration range of 1 to 9 mM of glucose was obtained as 5.8×10^{5} cm^3 mol^{-1} s^{-1}.

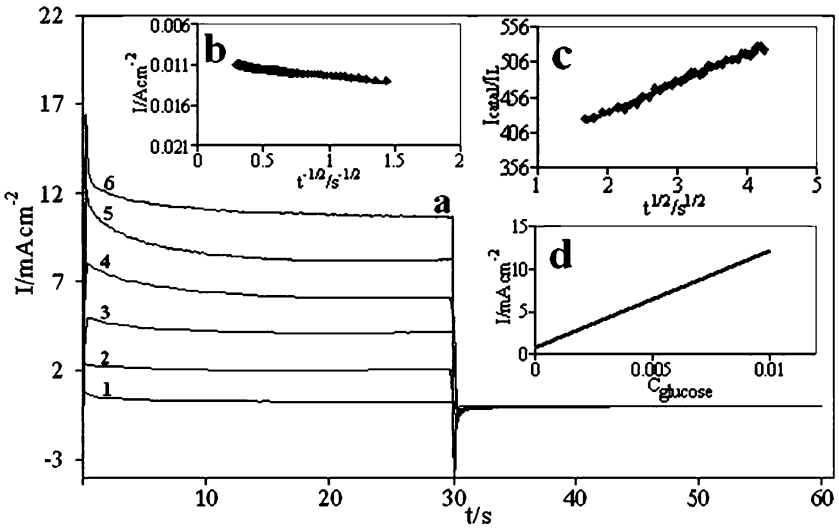

Fig. 9 **a** Double steps chronoamperograms of GC/NiCu electrode in 1 M NaOH solution with different concentrations of glucose of: 0 mM (*1*), 1 mM (*2*), 3 mM (*3*), 5 mM (*4*), 7 mM (*5*), and 9 mM (*6*). Potential steps were 560 and 320 mV, respectively. **b** Dependency of transient current on $t^{-1/2}$. **c** Dependence of $I_{\mathrm{catal}}/I_{\mathrm{L}}$ on $t^{1/2}$ derived from the data of chronoamperograms of *1* and *3* in panel **a**. **d** Plot of sampled transient current at fixed time of 10 s vs. glucose concentration

Figure 9d shows the plot of sampled current at fixed time (10 s) with respect to the concentration of glucose. A good linearity has been witnessed, and a limit of detection of 0.8 μM has been obtained from three times the standard deviation of the blank per the slope of calibration curve [47].

Conclusion

Nickel oxide film was formed electrochemically on electrodeposited nickel and nickel–copper alloy on a glassy carbon electrode in a regime of cyclic voltammetry and tested for the electro-oxidation of glucose in alkaline media. The addition of copper to the electrodeposited nickel is a very effective method of suppressing the formation of γ-NiOOH species during prolonged cycling processes in alkaline medium. Also from repeated cycling, it was observed that the overpotential for O_2 evolution increases for NiCu alloy modified electrode. The modified electrodes showed electrocatalytic activity for the oxidation of glucose at around 540 mV/Ag, AgCl, while the glassy carbon electrode presented no activity. More specifically, the response for glucose electro-oxidation at the NiCu alloy modified electrode are significantly larger than the response obtained for pure electrodeposited Ni. The anodic peak currents for glucose oxidation at GC/NiCu are linearly proportional to the square root of scan rate. Double steps choronoamperograms for the GC/NiCu in the presence of glucose show irreversible process, and the dominance of a diffusion-controlled process is evident. The diffusion coefficient of glucose has been obtained to be 1×10^{-5} cm^2 s^{-1}, in agreement with cyclic voltammetric response.

References

1. Essis LH, Beden B, Lamy C (1988) J Electroanal Chem 246:349. doi:10.1016/0022-0728(88)80171-2
2. Katz E, Willner I, Kotlyar AB (1999) J Electroanal Chem 479:64. doi:10.1016/S0022-0728(99)00425-8
3. Khoo SB, Yap MGS, Huang YL, Guo SX (1997) Anal Chim Acta 351:133. doi:10.1016/S0003-2670(97)00326-7
4. Johnson DC, Weber SG, Bond AM, Wightman RM, Shoup RE, Krull IS (1986) Anal Chim Acta 180:187. doi:10.1016/0003-2670(86)80007-1
5. Lei HW, Wu BL, Cha CS, Kita H (1995) J Electroanal Chem 382:103. doi:10.1016/0022-0728(94)03673-Q
6. Bagotzky VS, Vassilyev YB (1964) Electrochim Acta 9:869. doi:10.1016/0013-4686(64)85038-6
7. Bockris JO'M, Piersma BJ, Gileadi E (1964) Electrochim Acta 9:1329. doi:10.1016/0013-4686(64)87009-2
8. Bea IT, Xing X, Liu CC, Yeager E (1990) J Electroanal Chem 284:335. doi:10.1016/0022-0728(90)85043-5
9. Bae IT, Yeager E, Xing X, Liu CC (1991) J Electroanal Chem 309:131. doi:10.1016/0022-0728(91)87009-S
10. Popovic KD, Markovic NM, Tripkovic AV, Adzic RR (1991) J Electroanal Chem 313:181. doi:10.1016/0022-0728(91)85179-S
11. Zhao C, Shao C, Li M, Jiao K (2007) Talanta 71:1769. doi:10.1016/j.talanta.2006.08.013
12. Morita M, Niwa O, Tou S, Watanabe N (1999) J Chromatogr A 837:17. doi:10.1016/S0021-9673(99)00047-3
13. Wang J, Chen G, Chatrathi MP (2004) Electroanalysis 16:1603. doi:10.1002/elan.200302996
14. Hilmi A, Luong JHT (2000) Anal Chem 72:4677. doi:10.1021/ac000524h
15. Skou E (1977) Electrochim Acta 22:313. doi:10.1016/0013-4686(77)85079-2
16. Colon LA, Dadoo R, Zare RN (1993) Anal Chem 65:476. doi:10.1021/ac00052a027
17. Fleischmann M, Korinek K, Pletcher D (1972) J Chem Soc, Perkin Trans II 10:1396. doi:10.1039/p29720001396
18. Luo P, Zhang F, Baldwin RP (1991) Anal Chim Acta 244:169. doi:10.1016/S0003-2670(00)82494-0
19. Luo P, Prabhu SV, Baldwin RP (1990) Anal Chem 62:752. doi:10.1021/ac00206a021
20. Miller B (1969) J Electrochem Soc 116:1675. doi:10.1149/1.2411657
21. Marioli J, Luo P, Kuwana T (1993) Anal Chim Acta 282:571. doi:10.1016/0003-2670(93)80122-2
22. Marioli J, Kuwana T (1993) Electroanalysis 5:11. doi:10.1002/elan.1140050104
23. Khulbe KC, Mann RS, Manoogian A (1980) Chem Rev 80:417. doi:10.1021/cr60327a003
24. El-Shafei AA (1999) J Electroanal Chem 471:89. doi:10.1016/S0022-0728(99)00235-1
25. Briggs GWD, Snodin PR (1982) Electrochim Acta 27:565. doi:10.1016/0013-4686(82)85041-X
26. Hahn F, Beden B, Croissant MJ, Lamy C (1986) Electrochim Acta 31:335. doi:10.1016/0013-4686(86)80087-1
27. Desilvestro J, Corrigan DA, Weaver MJ (1988) J Electrochem Soc 135:885. doi:10.1149/1.2095818
28. Barnard R, Randell CF (1983) J Appl Electrochem 13:89. doi:10.1007/BF00615892
29. Conway BE, Liu TC (1987) J Chem Soc, Faraday Trans 83:1063. doi:10.1039/f19878301063
30. Druska P, Strehblow HH, Golledge S (1996) Corros Sci 37:835. doi:10.1016/0010-938X(96)00170-9
31. Luo P, Prabhu SV, Baldwin RP (1990) Anal Chem 62:752. doi:10.1021/ac00206a021
32. Bode H, Dehmelt K, Witte J (1966) Electrochim Acta 11:1079. doi:10.1016/0013-4686(66)80045-2
33. Schrebler Guzman RS, Vilche JR, Arvia AJ (1978) J Electrochem Soc 125:1578. doi:10.1149/1.2131247
34. Chen J, Bradhurst DH, Dou SX, Liu HK (1999) J Electrochem Soc 146:3606. doi:10.1149/1.1392522
35. Singh DJ (1998) J Electrochem Soc 145:116. doi:10.1149/1.1838222
36. Oshitani M, Watada M, Lida T (1995) In: Bennett PD, Sakai T (ed) Hydrogen and metal hydride batteries, The Electrochemical Society Proceedings Series. Pennington, NJ
37. Luo PF, Kuwana T, Paul DK, Sherwood PMA (1996) Anal Chem 68:3330. doi:10.1021/ac960236e
38. Bard AJ, Faulkner LR (2001) In: Bard AJ (ed) Electrochemical methods, fundamentals and applications. Wiley, New York
39. Laviron E (1979) J Electroanal Chem 101:19. doi:10.1016/S0022-0728(79)80075-3
40. Heli H, Jafarian M, Mahjani MG, Gobal F (2004) Electrochim Acta 49:4999. doi:10.1016/j.electacta.2004.06.015
41. Mho S, Johnson DC (2001) J Electroanal Chem 500:524. doi:10.1016/S0022-0728(00)00277-1

42. Nicholson RS, Shain I (1964) Anal Chem 36:706. doi:10.1021/ac60210a007
43. Harrison JA, Khan ZA (1970) J Electroanal Chem 28:131. doi:10.1016/S0022-0728(70)80288-1
44. Bard AJ, Faulkner LR (2001) In: Bard AJ (ed) Electrochemical methods, fundamentals and applications. Wiley, New York
45. Torto N, Ruzgas T, Gorton L (1999) J Electroanal Chem 464:252. doi:10.1016/S0022-0728(99)00041-8
46. Pariente F, Lorenzo E, Tobalina F, Abruna HD (1995) Anal Chem 67:3936. doi:10.1021/ac00117a019
47. Goyal RN, Gupta VK, Bachheti N (2007) Anal Chim Acta 597:82. doi:10.1016/j.aca.2007.06.017